Test and Analyses of a Bridge Continuous Composite Beam

Jean-Marie ARIBERT
Prof. des Universités
INSA
Rennes, France

Joël RAOUL
Ing. Ponts et Chaussées
SETRA
Paris, France

Olivier TERPEREAU
Assistant
INSA
Rennes, France

Summary

This paper deals with a test of a two-span continuous composite girder comprising sudden changes of cross-sections and mixed cross-sections (class 1 at mid-span and class 4 on internal support). Mainly the behaviour at serviceability limit state and ultimate limit state is presented. Also comparisons are made with different types of global analyses and with numerical simulation using a sophisticated software.

1. Introduction

In the frame of new concepts developed in Europe, particularly during the drafting of Eurocode 4 - Part 2 for composite bridges [1], some discrepancies with the French regulation [2] have appeared leading SETRA to order a two-span continuous composite beam test to INSA in Rennes. The loading procedure of this test has included several phases related to :

- the behaviour at serviceability limit state (non accumulation of deformations due to variable loads, cracking monitoring on the intermediate support) ;
- the resistance at ultimate limit state (maximum loads and possible redistribution of bending moments).

In parallel with this experimental approach, a specialized software has been developed on the basis of the finite element method specially adapted to the verification of composite bridge beams. This software is only used here for the simulation of the present test ; but in the future, it will be applied to the calibration of the various methods of analysis proposed in [1] covering a wider range of span lengths, different ratios between consecutive spans...

2. Test presentation

As shown in fig. 1, the tested composite beam comprises two continuous spans of 7.5 m and is subject to two independent concentrated loads P and Q each located at mid-span. This beam is class 1 at mid-span and class 4 on support A2 (due to the class 4 web). The bottom flange has a variable thickness (10 mm at mid-span, 15 mm on support A2) in order to simulate a composite bridge beam where the maximum resistance bending moments are reached almost simultaneously in sagging and hogging zones at ultimate limit state. Between the two loads, the web is heavily transversely stiffened to avoid a premature shear buckling.

The mechanical properties of the structural steel, reinforcement and concrete have been measured on several specimens leading to the characteristic values given in table 1.

	$f_y(MPa)$	$f_u(MPa)$
Web	480	570
10 mm flange	385	540
15 mm flange	465	585
Reinforcement	475	610

	$f_{cm}(MPa)$	$f_{ck}(MPa)$
Concrete	31.3	27.5

Table 1 . Material properties

Using these properties together with partial safety factors equal to 1, the mechanical properties of the composite cross-sections are as follows :

$I_1 = 12.3 \times 10^8$ mm^4 , $M^{+}_{pl.Rd} = 1166$ kN m in sagging moment regions ;

$I_2 = 7.4 \times 10^8$ mm^4 , $M^{-(eff)}_{el.Rd} = 935$ kN m in hogging moment regions.

During the casting of the slab, the steel beam was propped all along its length. The type of concrete was selected to minimize the effect of shrinkage ; so, the free shrinkage measured on an independent specimen of slab was equal to about 1×10^{-4} after one month. Due to this shrinkage and to the permanent loads, the stresses in structural steel and concrete have been estimated at −3.3 MPa (lower flange under load P) and + 1.2 MPa (concrete in tension over A2) respectively.

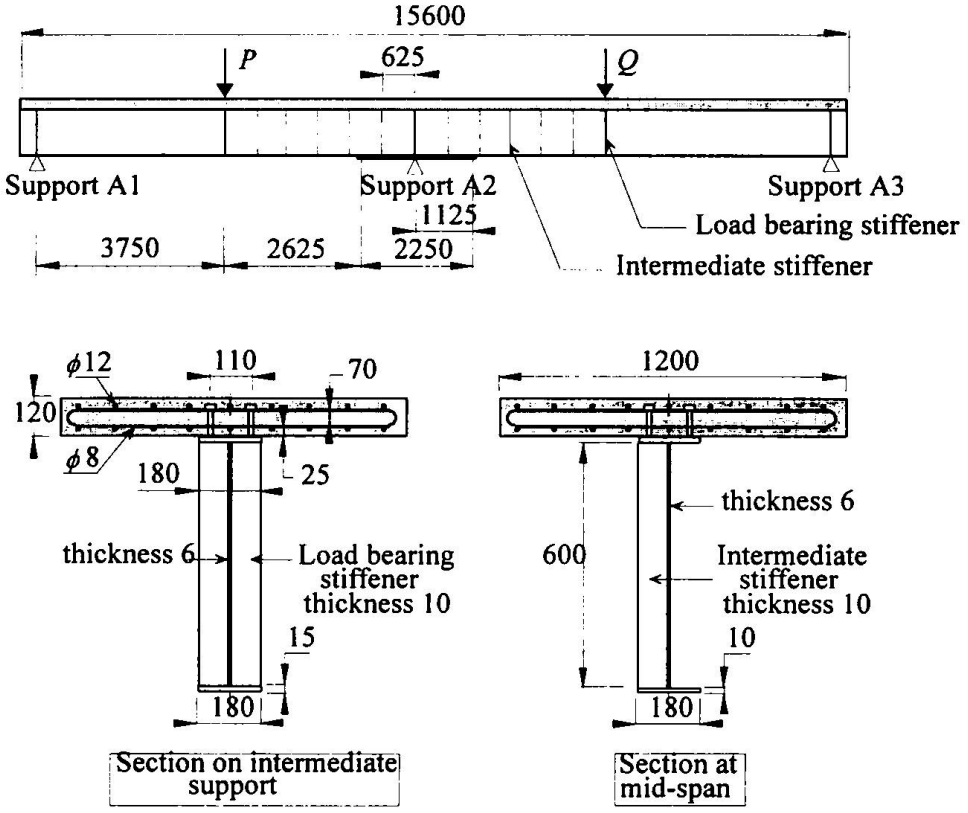

Fig. 1- Tested continuous composite beam

3. Test results and comparison with different types of analyses

The loading procedure comprises 123 phases. The main phases are summarized in table 2.

Table 2. Loading procedure

	Phase number	P(kN)	Q(kN)	Observation
	8	100	100	• First cracks (0.1 mm) in the slab over intermediate support
	14	400	400	• Cracks 0.2 mm
Serviceability limit state	19 to 29	5 cycles 400-450-400	400	
	30 to 39	5 cycles 400-475-400	400	
	40	500	400	• First plastification in the lower flange under P (cracks ≤0.3 mm)
	41 to 48	5 cycles 400-550-400	400	
	61 to 66	5 cycles 400-550-400	400	
Ultimate limit state	93 to 101	P = Q from 0 to 550		
	101 to 113	550 to 810	550	• Shear buckles over the support
	122	890	550	• Beam failure

Figure 2 shows the variation of the beam deflection at the loading point P. Figure 3 shows the variations of the bending moments at mid-span (loading point P) and over the intermediate support (point A2). These moments have been derived from measurements of the bearing reactions at supports A1 and A3. They have also been checked against strain gauges measures on the steel flanges near support A2.

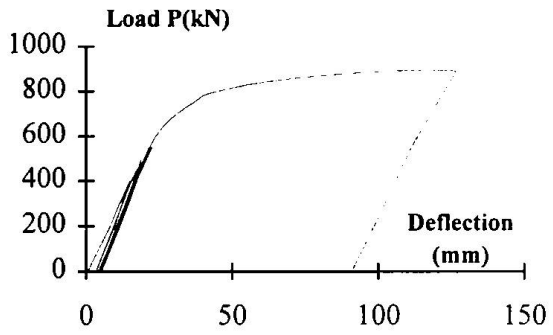

Fig.2 Load-deflection curve

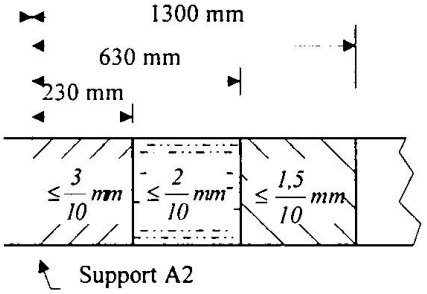

Fig.4 Distribution of crack widths

3.1. Serviceability limit state

(a) The first yielding appears during phase 40 for P = 500 kN and Q = 400 kN. A series of 5 cycles has been carried out around this loading (see table 2) and no cumulation of plastic deformation has been observed. But for phases 61 to 66 (P varying from 400 to 550), there is a more significant residual deflection (about 6% due essentially to the cracking of the slab obtained after the first cycle). This result tends to confirm the choice of a limitation of stresses of 1.0 f_y in the structural steel proposed in EC4-2 [1].

b) The crack widths have been carefully monitored up to phase 40 (S.L.S.). The reinforcement was designed according to EC4-1 [3] for a crack width of 0.3 mm. The distribution of the crack widths on each side of the intermediate support is shown in fig. 4.

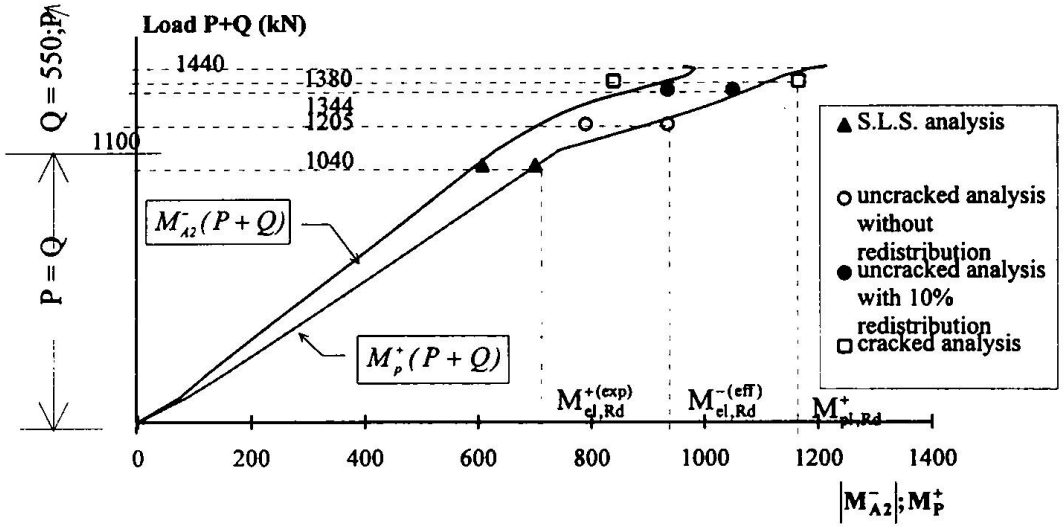

Fig.3 Variations of the bending moments at mid-span and over support A2

c) In fig. 3 related to the phases 93 to 122 (see table 2), the calculated bending moments at serviceability limit state have been plotted :

$M_P^+ = M_{el.Rd}^{+(exp)} = 701$ kNm (elastic bending resistance in the test condition) ;

$M_{A2}^- = -607$ kNm, for : $P = Q = 520$ kN.

Elastic analysis has been used adopting a cracked zone over 15 % of the span length on each side of support A2. The plotted points fit perfectly with the experimental curves.

3.2. Ultimate limit state

(a) Three types of analyses according to EC4.2[1] have been compared :

- an « uncracked » analysis without redistribution giving :

$$P_u^{(1)} = 655 \text{ kN} \quad , \text{ with : } M_{A2}^- = -935 \text{ kNm}, \; M_P^+ = 790 \text{ kNm}$$

- an « uncracked » analysis with a 10 % redistribution of the hogging bending moment at A2 leading to :

$$P_u^{(2)} = 794 \text{ kN} \quad , \text{ with : } M_{A2}^- = -935 \text{ kN m}, \quad M_P^+ = 1050 \text{ kN m}$$

- a « cracked » analysis as in 3.1.(c) giving :

$$P_u^{(3)} = 830 \text{ kN} \quad , \text{ with : } M_{A2}^- = -839 \text{ kNm} \quad , \quad M_P^+ = 1166 \text{ kNm}$$

All these calculated values of P_u are on the safe side in comparison with the experimental value $P_u^{(exp)} = 890$ kN. The high value of $P_u^{(exp)}$ is likely to have been allowed on account of redistribution of moments from mid-span to support A2. The points corresponding to the above analyses are plotted in fig. 3. In the present investigation, the « uncracked » analysis with a 10 % redistribution appears particularly appropriate whereas the « cracked » one tends to underestimate the bending moment on support A2.

(b) The shear plastic or buckling resistance has been verified in accordance with EC4.1[3] giving :

$V_{Rd} = V_{ba.Rd} = 680$ kN between A1 and P ;

$V_{Rd} = V_{pl.Rd} = 998$ kN between P and A2 (aspect ratio of the web panels of about 1).

That leads to a maximum ratio V_{Sd} / V_{Rd} of 0.57 close to 0.50. Consequently, the reduction of the calculated ultimate load P_u due to the vertical shear force is only 0.5 %.
(c) The connection was designed to resist the maximum possible shear flow at ultimate limit state (32 and 38 headed studs were welded between A1 and P and between P and A2 respectively, each having a shear resistance of about 100 kN).
(d) No lateral-torsional buckling has been observed during the test. But the calculation according to Annex B of EC4.1 (clause B.1.2) [3] would give $\bar{\lambda}_{LT} = 0.92$ and a reduction factor χ_{LT} of about 0.6 , what seems to be a paradox. The very good behaviour of the tested beam can only be explained by the presence of the high density of vertical stiffeners welded to both flanges and to the web. By spreading and adding their stiffness to the flexural stiffness k_2 of the web (such a method is not in EC4.1), $\bar{\lambda}_{LT}$ becomes 0.37 < 0.40, what leads to $\chi_{LT} = 1$.

4. Numerical simulation

A numerical model based on the finite element method has been developed at INSA in Rennes using specialized beam elements (for steel and concrete), shear connector elements and buckling elements [4]. This model has been generalized for composite bridge girders by introducing other possibilities such as gradual or sudden changes of cross-sections, local buckling of web in class 4 (by means of the concept of effective depth), tension stiffening in slab after the stage of stabilized crack formation, and creep of concrete allowing to take into account the sequence of construction (this last aspect is not concerned in the paper) [5]. The effect of tension stiffening has been formulated in accordance with Annex L of EC4.2 [1] expressing the average tensile force N_s of the slab versus the average strain ε_{sm} as shown in fig. 5 (with factor $\beta = 0.40$).

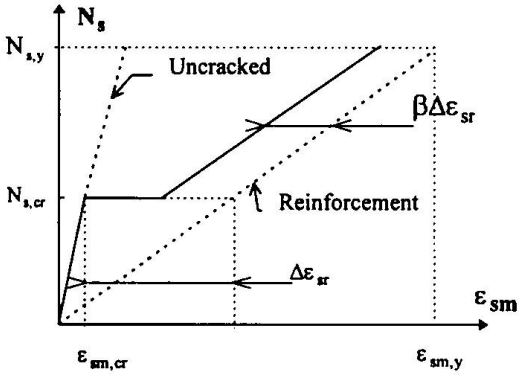

Fig.5 Tension stiffening curve

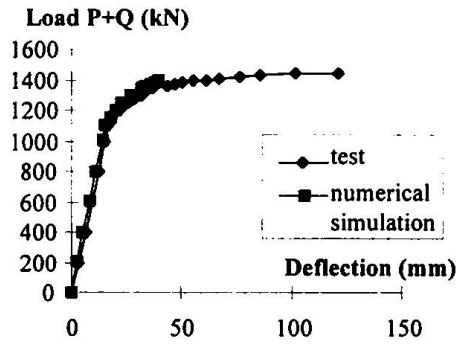

Fig.6 Comparison of the load-deflection curves

The composite beam tested above has been discretized using 186 finite beam elements and 68 shear connector elements. The simulated curve of the load versus the deflection (at the loading point P) is compared with the experimental one in fig. 6, showing a good agreement provided that a light additional deflection due to the vertical shear force in the web is taken into account for the elastic phase. Moreover, the simulated variations of the bending moments at mid-span and over support A2 are compared with the experimental ones (already given above) in fig. 7

and 8. But it is worth pointing out that the tension stiffening effect is only included in the simulation of fig. 7 and not in that of fig. 8. The better agreement in fig. 8 may appear a paradox though both simulations give the same ultimate load P_u. As explanation of such a paradox, it is possible to advance the gradual vanishing of tension stiffening during the test under the repeated cyclic loadings around the serviceability limit state. Also, some uncertainty of the real effective width of the slab in hogging moment zone may affect the results of the numerical simulation.

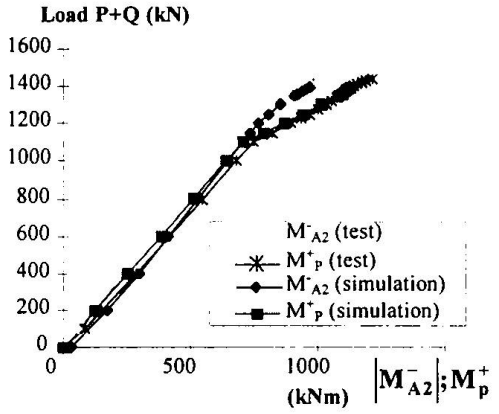

Fig.7 Comparison of load-bending moments curves (with tension stiffening)

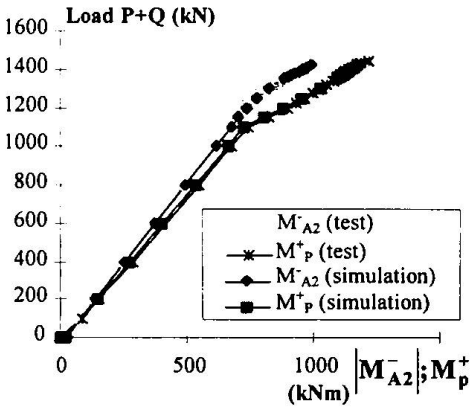

Fig.8 Comparison of load-bending moments curves (without tension stiffening)

5. Conclusion

The tested beam, representative of a composite bridge beam, confirms that the proposed methods to verify the serviceability limit state and the ultimate limit state in EC4-2 are safe and in rather good agreement with the experience. The software used for the numerical simulation gives results very close to the measured ones. It will be applied in the future to calibrate the analyses proposed in EC4-2 and to precisely define their scope.

References

1. Eurocode 4, « Design of composite steel and concrete structures », Part 2 : « Bridges », ENV 1994-2, Third draft, CEN, Brussels, January 1997.
2. Ministères de l'Urbanisme, du Logement, des Transports et de l'Environnement, « Circulaire n° 81-63 relativement au règlement de calcul des ponts mixtes acier-béton », 28 juillet 1981.
3. «Eurocode 4, « Design of composite steel and concrete structures », Part 1.1, « General rules and rules for buildings », ENV 1994-1-1, CEN, Brussels, 1994.
4. Aribert, J.M. , Ragneau, E., et Xu, H., « Developpement d'un élément fini de poutre mixte acier-béton intégrant les phénomènes de glissement et de semi-continuité avec éventuellement voilement local », Construction Métallique, N° 2, 1993.
5. Aribert, J.M., « Chapitre 8 : Modélisation des ouvrages mixtes acier-béton avec leur connexion », Volume 1, Calcul des ouvrages généraux de construction (AFPC - Emploi des éléments finis en génie civil), Hermès, Paris, 1997.